Mössbauer absorber detection of nuclear magnetic resonance at millikelvin temperature

G. A. Stewart,* W. D. Hutchison, S. J. Harker, and D. H. Chaplin
School of Physics, University College, UNSW, Australian Defence Force Academy, Canberra ACT 2600, Australia
(Received 2 September 2001; revised manuscript received 29 July 2002; published 16 October 2002)

A low-temperature experiment is reported in which the Mössbauer effect is used to monitor nuclear magnetic resonance in the $I=1/2$ ground state of ^{57}Fe. Contrary to an earlier attempt at this experiment the resonance is single line. Despite the enriched 30 at. % ^{57}Fe concentration of the iron foil specimen, the NMR line broadening is predominantly inhomogeneous in nature.

DOI: 10.1103/PhysRevB.66.134415 PACS number(s): 76.60.−k, 07.20.Mc, 61.18.Fs

I. INTRODUCTION

We report here the low-temperature Mössbauer detection of nuclear magnetic resonance (NMR) in the Mössbauer transition's own ground state. In this instance, it is the $I=1/2$ ground state of the well-known ^{57}Fe, 14.4 keV, Mössbauer transition that is considered for a thin foil specimen of high-purity iron, isotopically enriched to 30 at. % ^{57}Fe. The NMR line is found to be inhomogeneously broadened, even at this high^{57}Fe concentration, and frequency modulation is required to achieve signal saturation. This experiment should not be confused with the earlier work of Cain *et al.*[1,2] and Laurenz *et al.*,[3] which employed ^{57}Fe Mössbauer spectroscopy to monitor the NMR of the ^{57}Co, $I=7/2$, parent state.

This present type of experiment was first attempted at Monash University in the mid-1970's under much more difficult experimental conditions.[4] At that time Callaghan *et al.*[5] had demonstrated the existence of small nuclear quadrupole interactions at dilute radioactive probe nuclei using single-passage NMR on oriented nuclei (NMRON). This was despite the fact that the local iron site symmetry is cubic. It was conceivable that this same small interaction could be responsible for the small continuous-wave NMRON signals observed at the time. The Mössbauer experiment was one of several radiation detection techniques investigated in order to monitor low-temperature resonances without the influence of the nuclear quadrupole interaction (which is absent for the $I=1/2$ ground state of ^{57}Fe). The statistics were poor and the experimental results were regarded as too unreliable to publish. Nevertheless, there was some suggestion of a weak ^{57}Fe resonance that was split into two subresonances. If true, this was a puzzling phenomenon that this present experiment aimed to reexamine, under vastly improved cryogenic conditions.

The conventional continuous wave NMR signal, in low applied magnetic fields, is known to arise predominantly from nuclei within domain walls.[6] In contrast the Mössbauer-detected NMR (MNMR) technique employed here monitors the resonance of ^{57}Fe nuclei throughout the specimen. In this regard, the technique is more like NMRON whose signal is averaged over radioactive probe nuclei distributed throughout the system. As for NMRON, a small polarizing magnetic field is used here to align the domains and effectively eliminate any domain wall contributions. Under these conditions, it will be demonstrated that the Mössbauer-detected ^{57}Fe resonance is in fact a single-line resonance with a linewidth 2–3 times greater than that for a natural ^{57}Fe concentration in a powder specimen. A key point is that the ^{57}Fe probes are not chemical impurities. In this sense, the Fe host is not perturbed by the nondilute concentration of ^{57}Fe employed here. However, the nuclear spin-spin interaction within the ^{57}Fe ensemble could be expected to increase as the concentration is increased. Earlier measurements performed on a 95 at. % specimen, using NMR thermally detected via nuclear orientation (NMR-TDNO), yielded a homogeneously broadened resonance line.[7] In this work we report new thermally detected measurements on a 30 at. % specimen (with the same outcome) and offer an explanation for the apparent inconsistency between the two techniques.

Finally, the long relaxation times involved at low temperatures make it possible for the ^{57}Fe spin-lattice relaxation to be monitored directly using the same Mössbauer spectroscopy approach. This possibility is explored and the result compared with the current benchmark, the thermal cycling of oriented nuclei (TCON) work of Funk *et al.*[8]

II. TECHNIQUE

The basis of the low-temperature MNMR technique is shown in Fig. 1. The geometry is typical of any other ^{57}Fe Mössbauer absorber experiment[9] except that the absorber is cooled to millikelvin temperature and subjected to a weak radio frequency (rf) field. In this present experiment the ab-

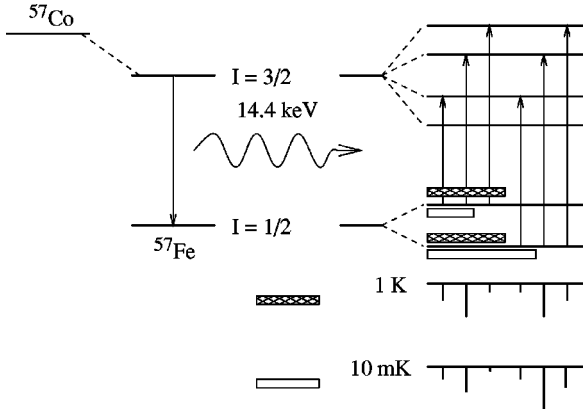

FIG. 1. The ^{57}Fe 14.4 keV transition and a schematic representation of the influence of temperature on its associated six-line Mössbauer spectrum (shown for the case of a polarizing field applied perpendicular to the γ path).

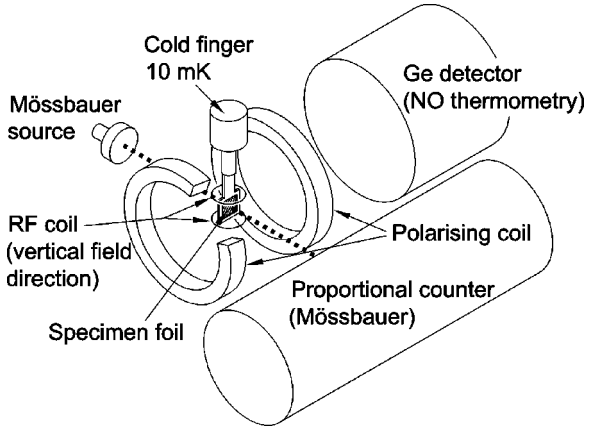

FIG. 2. Experimental geometry.

sorber specimen is a magnetized foil of iron enriched to 30 at. % ^{57}Fe (compared with the natural concentration of 2 at. %). Given that the splitting of the $I=1/2$ nuclear ground state corresponds to about 2 mK, in temperature units, the two sublevels are essentially equally populated at 1 K. The magnetically split, six-line Mössbauer spectrum 'tilts' when the specimen is cooled because the two sublevels are no longer equally populated. In principle, this phenomenon can be exploited as an *in situ* thermometer.[10] However, because it is complicated by the thickness effect,[11,12] nuclear orientation (NO) thermometry has also been employed here. The application of a low-power radio frequency field at the $I=1/2$ ground-state resonance frequency (approximately 46.5 MHz for ^{57}Fe in an iron host at $T\approx 0$K) tends to equilibrate the populations of the two sublevels and reduce the spectrum tilt. Thus the $I=1/2$ resonance is mapped out by monitoring the variation in tilt of the six-line Mössbauer spectrum as a function of frequency.

III. EXPERIMENTAL DETAILS

The geometry of the experiment is shown in Fig. 2. A 25 mCi ^{57}Co*Rh* source was mounted at room temperature outside the ^{3}He:^{4}He dilution refrigerator on a transducer which was driven with a sinusoidal motion. The specimen material (nominally 30 at. % ^{57}Fe) was prepared by reducing enriched Fe_2O_3 (95 at. % ^{57}Fe) under a flow of hydrogen and arc-melting the resultant metal with an appropriate amount of pure (4N8) natural iron. Repeated annealing and rolling produced a thin foil of dimension 10 mm$\times$10 mm $\times$1.9 μm which was diffused thermally with $\approx$2 μCi ^{60}Co activity for use as the NO thermometer. A larger activity would have contributed unnecessarily to thermal loading of the specimen (due to the absorption of emitted β radiation) and to the Mössbauer spectrum's background. The foil was soldered with indium to a 4.6μm thick Cu backing whose 1-mm-thick Cu frame was an integral part of the dilution refrigerator cold finger. The purpose of the thin copper backing was to promote a uniform temperature across the specimen foil with minimal reduction of transmitted γ intensity. The plane of the specimen foil was set perpendicular to the 14.4 keV γ-ray path, and the polarizing and rf fields were

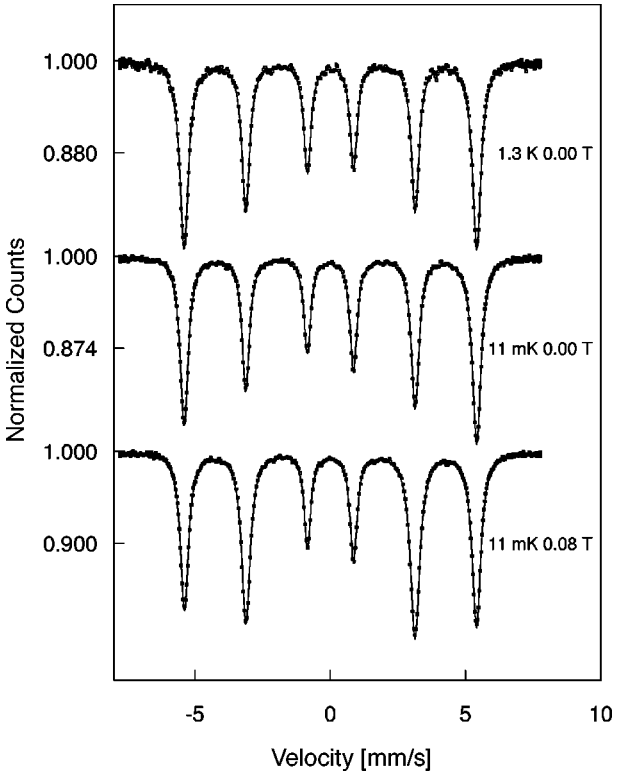

FIG. 3. Representative ^{57}Fe Mössbauer spectra in the absence of the rf field.

applied within the plane of the specimen foil but at right angles to one another. The intrinsic Ge detector used to monitor the ^{60}Coγ count rate (1178 keV and 1333 keV photopeaks) was positioned on the axis of the polarizing field. As shown in Fig. 2, this geometry requires a split-coil polarizing magnet. In order to minimize the γ path length through the cryostat, the coil radius needed to be as small as possible. To this end, the magnet was designed for a maximum field of just 0.5 T and the usual Helmholtz condition was relaxed to give an acceptable field inhomogeneity of $\leqslant$0.5% across the specimen volume. For a polarizing field of $B_{\rm pol}=0.1$ T, this inhomogeneity corresponds to $<$2% of the narrow conventional NMR linewidth for ^{57}Fe in natural Fe powder [full width at half maximum (FWHM) $\approx$30 kHz (Ref. 6)] and $<$0.05% of the ideal ^{57}Fe Mössbauer linewidth (FWHM ≈ 0.2 mm s^{-1}). The polarizing coil was calibrated at $9.309(4)\times 10^{-3}$ T/A using the known field dependence[13] of the NMRON frequency for ^{60}Co**Fe**. Finally, the cryostat dewars were modified to have rectangular tails with low attenuation Mylar ''windows'' along an eventual source-to-detector γ path of just 110 mm.

The recording of the Mössbauer spectra (typically of duration 3400 s) was synchronized with the programmed changes in the rf frequency and/or the frequency modulation (FM) amplitude. The FM frequency was fixed at 400 Hz. A 200 s wait time was programmed after each change of rf conditions to allow the system to approach equilibrium before acquisition of the next spectrum. Comparison of the upper two Mössbauer spectra in Fig. 3 illustrates the small degree of tilt that is achieved at a base temperature of 11 mK

(as determined by ^{60}Co*Fe* NO thermometry) and in the absence of an rf field. With the setting of the rf field level comes a trade-off between increased resonant signal and decreased tilt due to nonresonant heating of the specimen foil. For the spin-lattice relaxation measurements, the rf field frequency was switched from on resonance to off resonance and a sequence of 200 s Mössbauer spectra was recorded as the ^{57}Fe ensemble relaxed back to thermal equilibrium with the iron lattice. Because of the small MNMR signals that were achieved, it was always necessary to accumulate spectra over several 24 h spectrum acquisition cycles. In most cases, the spectra were analyzed in terms of six independent Lorentzian absorption lines with intensities I_i ($i=1$–6 from left to right as shown in Figs. 1 and 3). However, for the case of the transient spin-lattice relaxation data, the individual spectra were further analyzed in terms of an algorithm which made allowance for the thickness effect. For this purpose, a pulse-height spectrum of the 14.4 keV window was recorded for the *in situ* Mössbauer geometry and the photopeak was determined to be 75% of the transmitted radiation. Additional room-temperature Mössbauer spectra recorded for natural iron foils of decreasing thickness yielded an extrapolated ^{57}Fe*Rh* source linewidth of 0.117 mm/s.

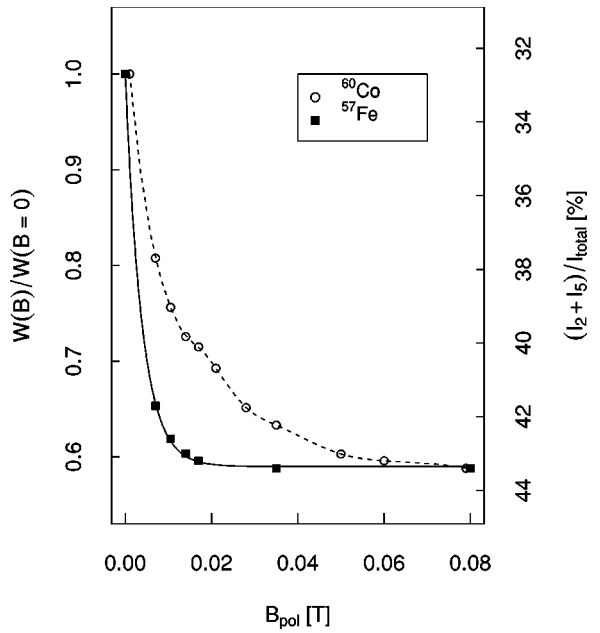

FIG. 4. ^{57}Fe Mössbauer spectroscopy intensity ratio $(I_2+I_5)/I_{\text{total}}$ (■) and normalized on-axis ^{60}Co γ anisotropy (○) as a function of the polarizing field B_{pol} during the initial magnetization of the specimen foil at 11 mK.

IV. RESULTS

A. Magnetization

The room-temperature Mössbauer spectrum was indicative of preferred magnetic alignment within the plane of the specimen foil (ideally $I_1:I_2:I_3=I_6:I_5:I_4=3:4:1$), a well-known consequence of repeated rolling and annealing.[14] However, once the specimen had been cooled to liquid helium temperature, the spectrum then more closely represented that expected for random magnetic orientation (ideally $I_1:I_2:I_3=I_6:I_5:I_4=3:2:1$) as observed in Fig. 3 for 1.3 K and 11 mK in the absence of an applied magnetic field. This phenomenon is presumably associated with strains that are set up in the cold foil. When the specimen was then magnetized from this initial random condition, a sequence of ^{57}Fe Mössbauer spectra and ^{60}Co γ count rates was recorded as B_{pol} was increased from 0 to 0.08 T. Whereas the ^{60}Co γ count rate is sensitive to alignment of the magnetic domains with respect to the polarizing field, the ^{57}Fe spectrum is sensitive to their alignment with respect to the γ path. In this sense, the two sets of results complement one another. As observed from the lower two spectra of Fig. 3, the intensities of the absorption lines 2 and 5 grow relative to the others as the specimen is magnetized. This is quantified in Fig. 4 where the ratio $(I_2+I_5)/I_{\text{total}}$ is seen to increase from $\approx$32% to $\approx$43.5%. The final value is less than the theoretical value of 50% expected for alignment of all domains perpendicular to the γ path. This is partly because allowance was not made for the thickness affect. There will also have been slight wrinkles in the thin foil surface. What is important is that the domains are already forced back into the plane of the foil at $B_{\text{pol}}\approx 0.02$ T. The ^{60}Co count rate exhibits a small shoulder at this same field but then dips further and converges on a minimum value at $B_{\text{pol}}\approx 0.08$ T. This suggests that the magnetization process proceeds in two stages: first the domains are forced into the plane of the foil and then they are aligned with the direction of the polarizing field. It should be noted that there is an additional effect retarding the approach to saturation of the γ anisotropy; this is a consequence of the γ anisotropy transforming under rotation as a predominantly second-rank tensor.

B. Resonances

For the purpose of mapping out the $I=1/2$, ^{57}Fe resonance, the tilt of the ^{57}Fe Mössbauer spectrum was defined as the ratio $R=(I_1+I_2+I_3)/(I_4+I_5+I_6)$. The first resonance (Fig. 5) was recorded for $B_{\text{pol}}=0.1$ T with FM$=\pm 30$ kHz at 400 Hz. The earlier Monash experiment[4] had suggested that the resonance might be split into two subresonances separated by $\approx$140 kHz. However, there is no evidence for such a splitting in these new, more accurate data. To test this result with increased frequency resolution and to test for a frequency shift with change of polarizing field, two further resonances (Fig. 6) were recorded for $B_{\text{pol}}=0.10$ T and 0.05 T with FM$=\pm 7$ kHz at 400 Hz. Again, there is no evidence for a split resonance. The dashed curves in Figs. 5 and 6 are the results of least-squares fits assuming a Gaussian line shape and a constant background. The fitted parameters (the central frequency f_0 and the raw FWHM linewidth Γ_{FWHM}) are collected in Table I. Also included in this table are the corresponding values of the effective hyperfine field B_{eff} at the ^{57}Fe nucleus and linewidths which have been corrected for the broadening influence of the FM. The B_{eff} values were calculated using the most recent value of $\mu(^{57}\text{Fe}, I=1/2)=+0.09044(7)\ \mu_N$.[15] Note that the uncertainty associated with this moment is the major contribution

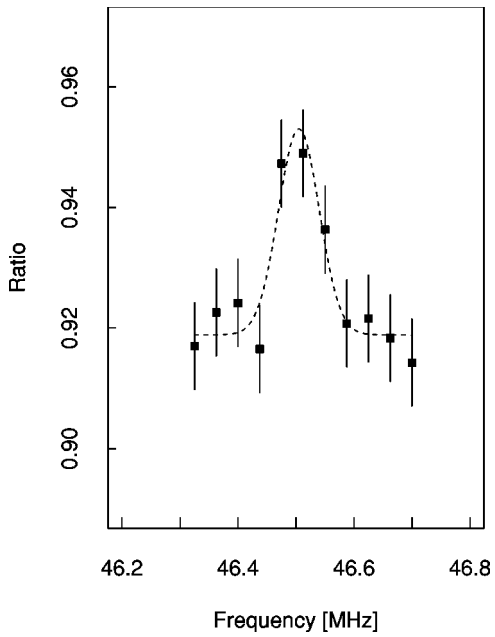

FIG. 5. The ^{57}Fe $I=1/2$ resonance obtained with $B_{pol}=0.1$ T and FM$=\pm 30$ kHz at 400 Hz. The fitted parameters are given in Table I.

(at least 70%) to the uncertainty quoted for each B_{eff}. Allowing for the Knight shift,[16] all three B_{eff} values are consistent with a hyperfine field of $B_{hf}=B_{eff}-B_{pol}\approx -33.83(3)$ T which is in close agreement with the accepted value of $B_{hf}\approx -33.82(3)$ T at 4.2 K (Violet and Pipkorn[17] modified to take account of the new value for the moment tabulated by Raghavan.[15])

The adjusted linewidths (right column of Table I) are in close agreement within experimental uncertainty, although there is some indication that the width decreases for the

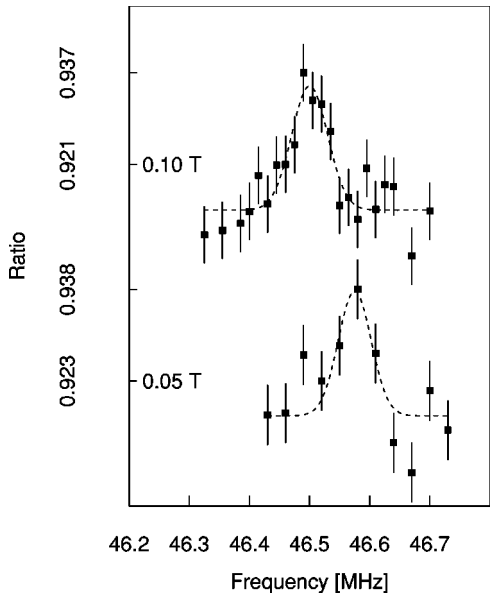

FIG. 6. The ^{57}Fe $I=1/2$ resonance obtained with FM$=\pm 7$ kHz at 400 Hz for $B_{pol}=0.10$ T and 0.05 T. The fitted parameters are given in Table I.

TABLE I. Parameters obtained by fits of a Gaussian line shape to the ^{57}Fe resonance.

FM [kHz]	B_{pol} [T]	f_0 [MHz]	B_{eff} [T]	Γ_{FWHM} [MHz] raw	adjusted
± 30	0.10	46.505(8)	$-33.729(32)$	0.083(19)	0.071(19)
± 7	0.10	46.500(6)	$-33.726(31)$	0.071(19)	0.070(19)
± 7	0.05	46.575(15)	$-33.780(37)$	0.064(39)	0.063(39)

smaller polarizing field. This is in keeping with a spread of demagnetizing fields associated with surface irregularities.[18] The weighted mean of 70(20) kHz corresponds to a hyperfine field spread of 0.051(15) T. This is almost 3 times larger than the linewidth of ≈ 24 kHz reported by Riedi[6] for domain wall nuclei in a specimen of natural iron powder at 4.2 K. Part of this increase in linewidth will be due to the spread of demagnetizing fields. However, the increased ^{57}Fe concentration might also be expected to play a role. Riedi commented that the resonance line was roughly a factor of 2 wider for a powder sample with 82.9 at. % ^{57}Fe. At the time, this was attributed to metal impurities in the enriched ^{57}Fe. However, energy dispersive spectroscopy (EDS) microprobe analysis of the present specimen material indicated that there was no significant impurity content (apart from the diffused ^{60}Co activity).

It is of interest to compare the present MNMR line width with the β-detected NMRON results of Ohtsubo *et al.*[19] (1996) for a 3 μm thick magnetized disc of dilute ^{59}Fe*Fe*. From Fig. 5 of their paper, the raw linewidth at 0.1 T is 89(7) kHz which adjusts to a value of 85(7) kHz when the FM broadening is stripped away. Allowing for the different g-factors of ^{59}Fe and ^{57}Fe these are very similar. However, the relevant ^{59}Fe, $I=3/2$ level is subject to a nuclear quadrupole interaction, the same type of weak quadrupole interaction that was observed first by Callaghan *et al.* for dilute ^{60}Co*Fe*. According to recent MAPON (modulated adiabatic passage on oriented nuclei) measurements,[20] this contributes significantly to the linewidth. Again, this points to additional line broadening for the present, enriched ^{57}Fe investigation (where $I=1/2$ and the quadrupole interaction can be ruled out). Given that the foil was backed by just 4.6 μm of copper (in contrast to being soldered to a solid stem), this additional line broadening is believed to have its origins in an increased spread of demagnetizing fields which is an inhomogeneous line broadening mechanism.

The relative importance of any homogeneous line broadening can be gauged from the influence of the FM amplitude on the resonance signal. The MNMR signal is defined as the percentage destruction of the Mössbauer spectrum tilt so that

$$\text{signal}[\%]=100\times\frac{[R_{\text{on-resonance}}-R_{\text{off-resonance}}]}{[1-R_{\text{off-resonance}}]}. \qquad (1)$$

It is evident from Figs. 5 and 6 that the MNMR signal increases substantially when the FM amplitude is increased from ± 7 kHz to ± 30 kHz. These two data are incorporated into Fig. 7 along with additional signals that were measured specifically for this purpose (i.e., without mapping out the

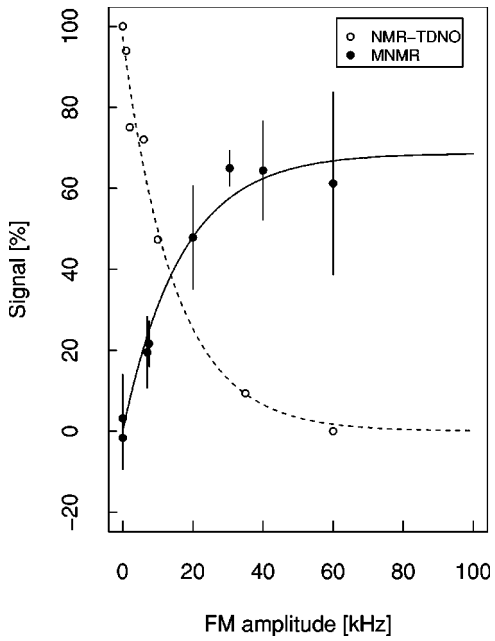

FIG. 7. Resonance signal as a function of FM amplitude for the 30 at. % foil at $B_{\mathrm{pol}}=0.1$ T [MNMR (●)] and for nuclear magnetic resonance thermally detected via nuclear orientation [NMR-TDNO (○)]. Note that the latter thermally detected signals have been normalized to 100% for the maximum signal.

full resonance). The solid curve in Fig. 7 is the predicted signal based on a Gaussian resonance line shape with the experimentally determined linewidth. The signal is then assumed to be proportional to the area under the Gaussian that is swept out by the frequency modulation. Based on these results, it would seem that the line broadening is predominantly inhomogeneous in nature.

This result, at first sight, seems to be in disaccord with previous observations for concentrated nuclear spins in magnetic systems at very low temperatures which show homogeneously broadened NMR lines. The Suhl-Nakamura interaction which couples nuclear spins via magnons (Ref. 21) is attributed as the dominant line broadening mechanism in such cases. For example, for manganese-based antiferromagnetic insulating compounds, the Suhl-Nakamura interaction can lead to ^{55}Mn NMR line broadening of several hundred kHz (Ref. 22) and is similarly dominant for ^{59}Co at natural (100%) abundance in ferromagnetic Co metal[23,24]. However it can be shown that the Suhl-Nakamura interaction is much weaker in the present ^{57}Fe***Fe*** case largely due to the extremely small ^{57}Fe nuclear moment. For a cubic ferromagnetic host the line broadening as stated by Suhl[25] (1968) is

$$h\Delta f_{\mathrm{FWHM}}=\left(\frac{I(I+1)}{6\pi}\right)^{1/2}\frac{A^2S}{g_{\mathrm{S}}\mu_{\mathrm{B}}B_{\mathrm{E}}}\left(\frac{B_{\mathrm{E}}}{B_{\mathrm{pol}}+B_{\mathrm{A}}}\right)^{1/4}, \quad (2)$$

where $A=\mu(I)B_{\mathrm{eff}}(\mathrm{sat})/IS$ is the hyperfine coupling constant for ^{57}Fe, B_{E} is the exchange field, B_{A} is the anisotropy field, and all other symbols have their usual meaning. Adopting values of $\mu(1/2)=0.09044\ \mu_N$, $B_{\mathrm{eff}}(\mathrm{sat})=33.82$ T, $I=1/2$, $S\approx 1$, $B_{\mathrm{E}}\approx 1000$ T, and $B_{\mathrm{pol}}+B_{\mathrm{A}}\approx 0.1$ T for ^{57}Fe***Fe*** we arrive at an estimated line broadening of $\Delta f_{\mathrm{FWHM}}\approx 0.2$ kHz, which is negligible compared with the present experimental linewidths of about 70 kHz. Clearly this calculation suggests that the spin-spin coupling is far weaker than the magnetic inhomogeneity present in the Fe foil and therefore correctly predicts the nature of the MNMR line. However, this contrasts with the NMR-TDNO work of Hutchison *et al.*[7] (1999) where, for a foil with 95 at. % ^{57}Fe concentration, a linewidth of similar magnitude to the MNMR was obtained but without the need for FM. In fact, the introduction of FM, with increasing amplitude, led to its complete suppression, implying a homogeneously coupled line. The difference in ^{57}Fe concentration between the two experiments is of course a clouding issue. Therefore it was decided to record additional NMR-TDNO data for a specimen with the same 30 at. % ^{57}Fe concentration as for the present MNMR measurements. These new results were recorded with the same applied field of $B_{\mathrm{pol}}=0.1$ T and are virtually indistinguishable from the results obtained earlier for the higher 95 at. % ^{57}Fe concentration.[7] The dependence of the NMR-TDNO signal on FM amplitude is shown in Fig. 7 (open circles). These data remain in clear disagreement with the present MNMR results and it is evident that the contrasting behavior has to result from a difference between the two experiments.

Although the two techniques MNMR and NMR-TDNO utilize different detection methods, there is nothing intrinsic to either that can lead to the contrasting NMR line broadening as observed. The two experiments were performed on the same cryostat but with different rf coil and cold finger configurations. The key difference appears to be the likely strength of the rf field at the iron foils in the two cases. The ^{57}Fe***Fe*** system is somewhat unique in its combination of a relatively narrow resonance line, slow nuclear spin-lattice relaxation, and negligible nuclear spin-spin coupling which all combine to allow the possibility that a modest increase in rf strength could transform the observed resonance line from an inhomogeneously broadened one in the MNMR case to a rf (power-) broadened homogeneous line in the NMR-TDNO experiments.

C. ^{57}Fe spin-lattice relaxation

On the basis of the reasonably strong MNMR signals observed above, it was decided to monitor the nuclear spin-lattice relaxation of the ^{57}Fe, $I=1/2$ sublevel populations. For these measurements, the polarizing field was set at $B_{\mathrm{pol}}=0.1$ T. At the commencement of each measurement cycle, the signal was saturated on resonance with FM$=\pm 40$ kHz at 400 Hz. Next, the FM was switched off and the rf shifted to off resonance, while a sequence of 100 s and 200 s duration Mössbauer spectra was recorded and added to those from the previous cycle. The corresponding ratios R (derived from simple fits of six Lorentzian lines) are plotted in Fig. 8 as solid squares. Also plotted as open squares in Fig. 8 are the inverse spin temperatures $\beta=1/T_s$, corresponding to corrected ratios derived from a full spectrum analysis with allowance for the thickness effect. This type of analysis was first tested against the final two spectra of Fig. 3 (for which

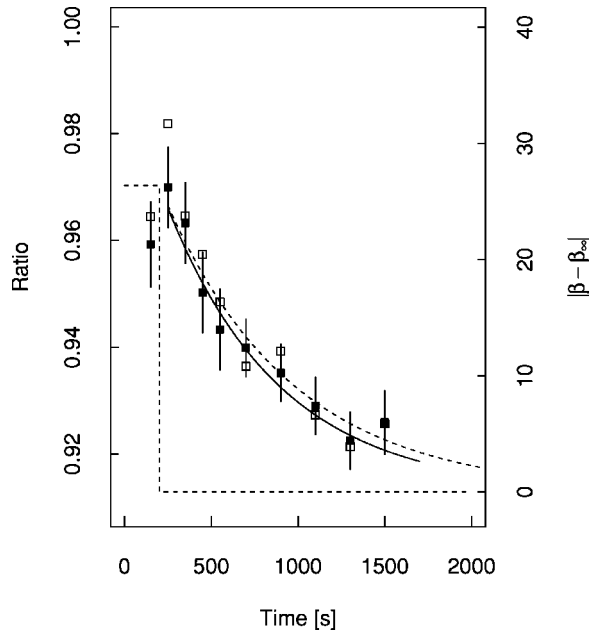

FIG. 8. Nuclear spin-lattice relaxation observed for $B_{\mathrm{pol}}=0.1$ T using ratios calculated from six-Lorentzian fits to the ^{57}Fe Mössbauer spectra (■) and inverse spin temperature $\beta=1/T_s$ obtained from full thickness effect analyses (□). The rf sequence was on-resonance FM$=\pm 40$ kHz at 400 Hz, followed by off-resonance with no FM.

no rf was applied) and yielded temperatures of 10.6 mK and 12.9 mK, respectively, compared with the 11.0 mK from the ^{57}Fe NO thermometry.

The ratio of the populations of a two-level system can always be described in terms of a spin temperature whose time dependence during spin-lattice relaxation is given by

$$\beta(t)-\beta(\infty)=[\beta(0)-\beta(\infty)]\times \mathrm{e}^{-t/T_1}, \tag{3}$$

where T_1 is the nuclear spin-lattice relaxation time. In this equation, $t=\infty$ corresponds to $T_S=T_L$, the base lattice temperature under the influence of the off-resonance rf heating. The horizontal dashed lines in Fig. 8 represent the initial and final conditions already determined from the spectra recorded for FM$=\pm 40$ kHz in Fig. 7. With these values fixed, the only free parameter is T_1. In the linear approximation ($\beta \propto \ln R \approx 1-R$ for $R \approx 1$), the time dependence of β [Eq. (3)] should also apply for the ratio R. Least-squares fits then yield values of $T_1=651(33)$ s for the six-Lorentzian R data (solid curve in Fig. 8) and $T_1=730(110)$ s for the spin temperature analysis (dashed curve in Fig. 8).

The full spectrum analysis (allowing for thickness) yielded the base temperature with off-resonance rf heating as $T_L=23(1)$ mK compared with $T_L=17.7(5)$ mK from the ^{60}Co NO thermometry. The Berlin group has applied thermal cycling of oriented nuclei to T_1 determination[8] for an extensive range of impurity-host combinations and this technique represents the current benchmark against which other measurements can be tested. If we adopt the ^{60}Co lattice temperature of 17.7(5) mK as the more reliable in the present case then, for $B_{\mathrm{pol}}=0.1$ T, the thermal cycling results for 95% ^{57}Fe (Ref. 8) predict a faster nuclear spin-lattice relaxation time of $T_1=420$ s. It is generally accepted that the ^{57}Fe concentration should have no influence on T_1. Nuclear spin-lattice relaxation is dependent on the density of electron states at the host Fermi level, and ^{57}Fe is an isoelectronic probe. A closer T_1 prediction would require a base temperature of 11 mK, as was observed here in the absence of rf heating (final two spectra of Fig. 3). Given that the ^{60}Co activity was diffused into the central region of the specimen foil, the discrepancy might be explained by the existence of an rf-induced temperature gradient across the thin foil specimen. Another issue is the reliance on predetermined initial and final temperatures for the present T_1 determination. We note that it is notoriously difficult to determine experimental T_1 values from nuclear spin-lattice relaxation curves where the initial conditions are established using continuous-wave rf excitation.[26] The present $I=1/2$ case is greatly simplified because the relative populations of the two sublevels can always be described in terms of a trivial Boltzmann population and associated spin temperature. Smaller T_1 values were obtained when the predetermined initial and final temperatures were treated as free variables. The advantage of the TCON technique is that the applied rf is used only for nonresonant heating of the specimen.

V. CONCLUSIONS AND FUTURE WORK

With improved statistics, this new experiment has demonstrated that the ^{57}Fe, $I=1/2$, NMR can be detected using the Mössbauer effect and that the resonance is *not* split. In addition, it has been shown that MNMR can be used to monitor the spin-lattice relaxation of the ^{57}Fe nuclei.

The counterintuitive outcome of inhomogeneous line broadening being dominant for such a high ^{57}Fe concentration has led to a reappraisal of the related thermally detected NMR measurements. It is proposed that the homogeneous line broadening observed using NMR-TDNO is a consequence of rf power broadening. Further NMR-TDNO measurements are currently underway to verify the role of rf strength and check what role, if any, ^{57}Fe concentrations may play.

ACKNOWLEDGMENTS

The authors thank Liam Waldron for his assistance with specimen preparation and polarizing coil design, Vernon Edge for specimen preparation, and Fred Johnson for assistance with the SEMS specimen analysis at the ANU's Research School of Biological Science and for assistance with diagrams. The School of Physics' mechanical workshop was responsible for the extensive modifications of the ^{3}He/^{4}He dilution refrigerator. John Barclay, John Cashion, Paul Clark, and Peter Blamey are acknowledged for their contributions to the earlier Monash experiment. This work was supported by an ARC Small Grant and a University College Special Research Grant.

*Electronic address: g.stewart@adfa.edu.au; http://www.ph.adfa.edu.au/g-stewart/

[1] C.J. Cain, Phys. Lett. **38A**, 279 (1972).
[2] C.J. Cain, J.A. Barclay, and J.D. Cashion, J. Low Temp. Phys. **19**, 513 (1975).
[3] R. Laurenz, E. Klein, and W.D. Brewer, Z. Phys. **270**, 233 (1974).
[4] G. A. Stewart, Ph.D. thesis, Monash University, 1976.
[5] P.T. Callaghan, P.D. Johnston, and N.J. Stone, J. Phys. C **7**, 3161 (1974).
[6] P.C. Riedi, J. Phys. F: Met. Phys. **5**, 186 (1975).
[7] W.D. Hutchison, S.J. Harker, D.H. Chaplin, T. Funk, and E. Klein, Hyperfine Interact. **120-121**, 193 (1999).
[8] T. Funk, E. Klein, and W.D. Brewer, Phys. Lett. A **248**, 457 (1998).
[9] *Mössbauer Spectroscopy I*, edited by U. Gonser, Vol. 5 of *Topics in Applied Physics* (Springer-Verlag, Berlin, 1975).
[10] G. M. Kalvius, T. E. Katila, and O. V. Lounasmaa, in *Mössbauer Effect Methodology*, edited by I. J. Gruverman (Plenum Press, New York, 1970), Vol. 5, pp. 231–267.
[11] M. C. D. Ure and P. A. Flinn, in *Mössbauer Effect Methodology*, edited by I. J. Gruverman, C. W. Seidel, and D. K. Dieterly (Plenum Press, New York, 1971), Vol. 7, pp. 245–262.
[12] G. K. Shenoy, J. M. Friedt, H. Maletta, and S. L. Ruby, in *Mössbauer Effect Methodology*, edited by I. J. Gruverman, C. W. Seidel, and D. K. Dieterly (Plenum Press, New York, 1974), Vol. 9, pp. 277–305.
[13] H.R. Foster, D.H. Chaplin, D.E. Swan, B.G. Turrell, and G.V.H. Wilson, Hyperfine Interact. **10**, 1149 (1981).
[14] R. M. Bozorth, *Ferromagnetism* (Van Nostrand, New Jersey, 1951).
[15] P. Raghavan, At. Data Nucl. Data Tables **42**, 189 (1989).
[16] A. Oppelt, N. Kaplan, D. Fekete, and N. Kaplan, J. Magn. Magn. Mater. **15-18**, 660 (1980).
[17] C.E. Violet and D.N. Pipkorn, J. Appl. Phys. **42**, 4339 (1965).
[18] R. Kieser, N. Kaplan, and B.G. Turrell, Phys. Rev. B **9**, 2165 (1974).
[19] T. Ohtsubo, D.J. Cho, Y. Yanagihashi, S. Ohya, and S. Muto, Phys. Rev. C **54**, 554 (1996).
[20] W. D. Hutchison, D. H. Chaplin, S. Ohya, S. Muto, K. Nishimura, H. Sato, Y. Kawamura, and A. E. Stuchbery, Phys. Rev. B (to be published).
[21] E. A. Turov and M. P. Petrov, *Nuclear Magnetic Resonance in Ferro-and Antiferromagnets* (Wiley, New York, 1972).
[22] B.G. Turrell, Hyperfine Interact. **120-121**, 13 (1999).
[23] M. Willets, M. LeGros, A. Kotlicki, G. Eska, C.E. Johnson, and B.G. Turrell, Czech. J. Phys. **46 S4**, 2167 (1996).
[24] G. Seewald, E. Hagn, and E. Zech, Phys. Lett. A **220**, 287 (1996).
[25] H. Suhl, Phys. Rev. **109**, 606 (1958).
[26] E. Klein, in *Low-Temperature Nuclear Orientation*, edited by N. J. Stone and H. Postma (North-Holland, Amsterdam, 1986), Chap. 12, p. 612.